

BER Degradation by Signal-Reshaping Processors With Noninstantaneous Response

Taras I. Lakoba

Abstract—We show analytically that if the response of a signal-reshaping processor is slower than (or comparable to) the time scale of variations of the temporal profile of the input signal, then such a processor necessarily degrades the signal's bit error rate (BER). Here, the BER comparison is made for the cases where the receiver is placed immediately before and immediately after the processor. As primary examples of such processors, we consider all-optical 2R (reamplification and reshaping) regenerators, but also mention that the aforementioned BER degradation can occur in wavelength converters and electronic components of the receiver.

Index Terms—All-optical regeneration, digital signal processors, optical communication, optical fiber communication, optical signal detection, optical signal processing, signal detection, signal processing, transfer functions.

I. INTRODUCTION

A number of devices proposed for all-optical signal processing rely on pulse propagation in a nonlinear medium (such as fiber or semiconductor) with noninstantaneous response, where the latter occurs either due to chromatic dispersion or filtering (in fibers) or due to finite carrier recombination time (in semiconductors). In this paper, we will mainly refer to all-optical 2R (reamplification and reshaping) regenerators (see, e.g., [1]–[3]) as examples of such devices; however, our main result will also apply to, e.g., wavelength converters [4]–[7], as well to as other (not necessarily all-optical) signal processors. Often (see, e.g., [1], [3], and [8]), researchers model signals entering the regenerator as having the same shape and width but variable peak powers. Then the output signal power depends only on the input power, and this dependence is sometimes referred to as the static transfer function. In such an approach, the regenerator is considered as being fully characterized by its static transfer function. However, due to the interplay between the nonlinearity and time-dependent response of the device, the signal output power depends not only on the input power, but also on the signal's temporal profile. That is, signals with a given value of received power in the absence of a regenerator have a continuum of different shapes, and, therefore, they will have not a unique power, but a distribution of powers, at the output of the regenerator. This is illustrated in Fig. 1, where

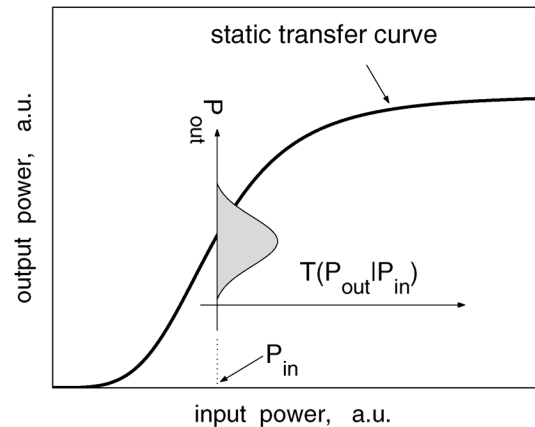


Fig. 1. Schematics of the static power transfer curve and of the distribution $T(P_{\text{out}}|P_{\text{in}})$ of output powers. This distribution is caused by the fact that input signal samples with the same peak power P_{in} have a continuous distribution of temporal shapes.

such a distribution is shown only for one value of the “input” power. Thus, there must exist situations where modeling of the regenerator’s action by its static power transfer function would lead to inaccurate results. Indeed, it was recently reported [3], [9], [10] that this is the case for the bit error rate (BER) estimation at the output of a single 2R regenerator. Namely, the authors of [3] and [10] showed that modeling the transformation of a noisy signal in a regenerator using a static transfer function would falsely predict BER values that are two-three orders of magnitude better (i.e., lower) than those actually obtained.

In Section II of this paper, we will provide an analytical base for the BER-related results of [3] and [10]: We will prove that if at the output of the signal processor, logical ONES and logical ZEROS have the *same* distribution of powers $T(P_{\text{out}}|P_{\text{in}})$ (see Fig. 1), then the BER after such a processor is worse (i.e., higher) than that immediately before it. (As explained, e.g., in [10]–[12], a *chain* of regenerators distributed along the transmission line will still be able to improve the BER at the receiver placed at the end of the line.) In Section III, we will explain that for a realistic case where those power distributions for ONES and ZEROS are different but considerably overlap, the BER is still degraded by the signal-reshaping processor. We will also point out that, in light of this result, a signal-retiming or phase-restoring processor placed in front of the receiver *can* improve the BER. We will draw conclusions in Section IV.

II. PROOF OF THE MAIN RESULT

In this section, we will use regenerators as a specific example of signal processors with noninstantaneous response. In the next section, we will discuss how the BER degradation manifests itself in other types of such processors.

Manuscript received June 06, 2008; revised September 30, 2008 and January 15, 2009. First published April 28, 2009; current version published May 08, 2009. This work was supported in part by the National Science Foundation under Grant DMS-0507429.

The author is with the Department of Mathematics and Statistics, University of Vermont, Burlington, VT 05401 USA (e-mail: lakobati@cems.uvm.edu).

Digital Object Identifier 10.1109/JLT.2009.2014976

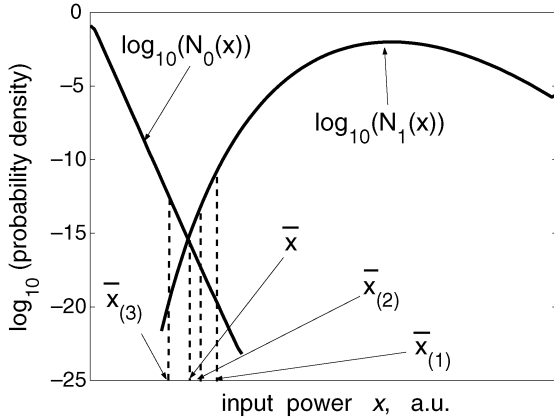


Fig. 2. Schematics of probability densities of ZEROs and ONES. The optimum threshold \bar{x} and “partial thresholds” $\bar{x}_{(m)}$ are defined in (2) and (15), respectively. The “partial thresholds” are also shown in Fig. 4.

A. Preliminaries

Let x and y be the powers, detected by the receiver, of signals at the input and output of the regenerator, respectively. If the regenerator’s response were instantaneous, then one would have $y = f(x)$, where $f(x)$ is the static transfer function of the regenerator. When $f(x)$ is a monotonic¹ function for all x , it is known (see, e.g., [13]) that the BERs of x and y are the same. Here, we will briefly outline the proof of this statement, as its steps will be repeated in the proof of our main result. The BER of x is computed as

$$\text{BER}_x = \frac{1}{2} \int_0^{\bar{x}} N_1(x) dx + \frac{1}{2} \int_{\bar{x}}^{\infty} N_0(x) dx \quad (1)$$

where the “1/2” is the probability of receiving a ZERO or a ONE, $N_{0,1}(x)$ are the respective probability densities that the received *nonregenerated* symbol (ZERO or ONE) has power x , and the threshold \bar{x} is found from the condition that BER_x be at its minimum. The latter condition yields

$$\frac{d}{d\bar{x}} \text{BER}_x = 0 \Rightarrow N_1(\bar{x}) = N_0(\bar{x}). \quad (2)$$

We assume (and in all cases known to us it is true) that the solution \bar{x} of (2) is unique (see Fig. 2).

Now let $R_{0,1}(y)$ be the probability densities of the *regenerated* ZEROs and ONES, respectively. Then the BER of y is

$$\text{BER}_y = \frac{1}{2} \int_0^{\bar{y}} R_1(y) dy + \frac{1}{2} \int_{\bar{y}}^{\infty} R_0(y) dy \quad (3)$$

where \bar{y} satisfies the counterpart of (2)

$$\frac{d}{d\bar{y}} \text{BER}_y = 0 \Rightarrow R_1(\bar{y}) = R_0(\bar{y}). \quad (4)$$

Since y and x are related by an algebraic relation $y = f(x)$, one has

$$R_k(y) dy = N_k(x) dx, \quad k = 0, 1. \quad (5)$$

¹For definiteness, we will now assume that $f(x)$ is increasing, but will relax the monotonicity condition later on.

Substituting this into the last equation in (4), one obtains

$$N_1(f^{-1}(\bar{y})) = N_0(f^{-1}(\bar{y})) \quad (6)$$

where $f^{-1}(y)$, the inverse of $f(x)$, exists since $f(x)$ is monotonic. Comparing (6) with (2), one concludes that

$$\bar{x} = f^{-1}(\bar{y}), \quad \text{or} \quad \bar{y} = f(\bar{x}). \quad (7)$$

Substituting (5) and (7) into (3), one verifies that $\text{BER}_y = \text{BER}_x$.

Let us make two remarks about this derivation. First, the condition that $f(x)$ is strictly monotonic (e.g., increasing) may not hold for a particular regenerator (see, e.g., [1], [9], and [10]). However, all that is really required is that $y = f(x)$ be an invertible (i.e., a one-to-one) function *near the threshold* \bar{y} . This condition holds for any regenerator considered for practical use.

Second, we stress that the key relation which allowed us to derive that $\text{BER}_y = \text{BER}_x$ for the regenerator with *instantaneous* response was (7), which in turn was made possible by the *local* relation (5) between $N_k(x)$ and $R_k(y)$.

Now, for a regenerator with *non-instantaneous* response, the counterpart of (5) is a nonlocal, integral relation

$$R_k(y) = \int_0^{\infty} N_k(x) T(y|x) dx. \quad (8)$$

Here $T(y|x)$ is the conditional probability density that a non-regenerated signal with received power x is transformed by the regenerator into a signal with received power y . In Fig. 1, it is denoted as $T(P_{\text{out}}|P_{\text{in}})$. Note that the information about the entire complex evolution of a signal with arbitrary shape is “lumped” into the input-output function $T(y|x)$ of only two variables. This is adequate because the input and output received powers x and y are the only variables that the receiver “knows about”. Let us also mention that the projection of the 2-D surface $T(y|x)$ onto the (x, y) -plane appears as a curved band enclosing the static transfer curve $y = f(x)$. For this reason, we will refer to $T(y|x)$ as a “transfer band” of the regenerator. Such transfer bands for ZEROs and ONES, obtained numerically for a regenerator considered in [10], are shown in Fig. 3. Specifically, this figure illustrates the situation where the shape of the signal varied due to noise added to the “clean” input, with the bandwidth of the noise being about twice that of the “clean” pulses.

Note that $T(y|x)$ must satisfy the normalization condition

$$\int_0^{\infty} T(y|x) dy = 1 \quad (9)$$

which means that the input power x is transformed by the regenerator into *some* power y .

Our goal is to prove that unless $T(y|x) = \delta(y - f(x))$, which would imply (5), the BER is degraded by the regenerator

$$\text{BER}_y > \text{BER}_x. \quad (10)$$

We will first prove this for a particular form of $T(y|x)$ where this transfer band consists of a finite set of isolated transfer curves

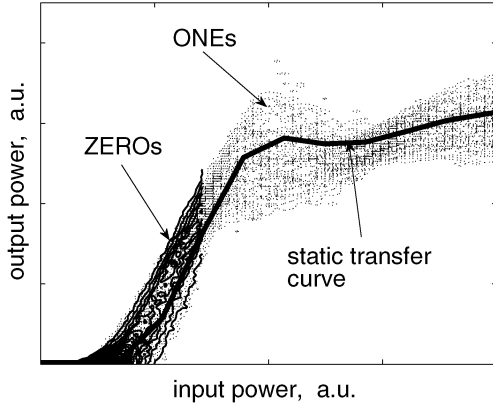


Fig. 3. Contour plots of the conditional probability densities $T(y|x)$ obtained separately for ZEROs and ONEs for a regenerator considered in [10].

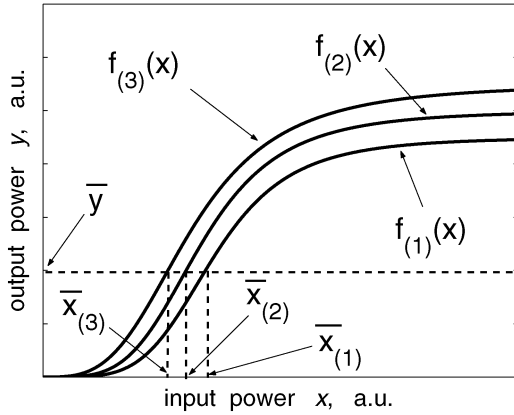


Fig. 4. Schematics of transfer curves f_m , $m = 1, 2, 3$, and the corresponding “partial thresholds” \bar{x}_m defined by (15).

$$T(y|x) = \sum_{m=1}^M a_m \delta(y - f_m(x)), \quad \sum_{m=1}^M a_m = 1. \quad (11)$$

Equation (11) specifies that an input signal with power x is transformed by the regenerator into a signal having one of the powers $y_m \equiv f_m(x)$ with probability a_m . This is illustrated in Fig. 4. Here and below the subscript in parentheses, as in a_m , $m = 1, \dots, M$, refers to the m th curve, while the subscript without parentheses, as in $N_k(x)$, $k = 0, 1$, distinguishes between the logical symbols ZERO and ONE.

We include the proof of (10) for the restricted form (11) of $T(y|x)$ because: i) this proof will clearly show the reason behind the BER degradation and ii) it will also show how the proof in the general case could be constructed. The reader who is not interested in mathematical details may skip to the last paragraph of Section II-B for an informal interpretation of this proof.

Let us note that the situation where the action of a 2R regenerator was described by a set of discrete transfer curves, as in (11), was considered in [11]. There, the “splitting” of the single transfer curve into a set occurred due to bit-pattern dependence: the power of a pulse at the output of a regenerator was influenced by the pulse’s interaction inside the device with its “neighbors”

in adjacent bit slots. The authors of [11] demonstrated numerically the BER degradation at the regenerator’s output due to this bit-pattern dependence, but they did not explicitly explain the mechanism of that degradation. We will describe this mechanism in the next subsection.

B. Proof of (10) for $T(y|x)$ Given by (11)

We assume that the functions $f_m(x)$ in (11) satisfy two conditions

$$\frac{df_m}{dx} > 0 \Leftrightarrow \frac{df_m^{-1}}{dy} > 0, \quad m = 1, \dots, M \quad (12a)$$

$$f_m(x) > f_j(x), \quad \text{for } x > 0 \text{ and } m > j. \quad (12b)$$

The first of these conditions is a counterpart of the condition that the static transfer function $f(x)$, used in the derivation above, be monotonic. As noted after (7), this condition needs to hold only near the threshold \bar{y} to guarantee that $f_m^{-1}(y)$ exist. The second condition simply says that different curves $f_m(x)$ do not intersect, except possibly at $x = 0$ (see Fig. 4).

Following the steps of the derivation found in Section II-A, we will obtain a counterpart of the key relation (7). Substitution of (11) into (8) yields

$$R_k(y) = \sum_{m=1}^M a_m N_k \left(f_m^{-1}(y) \right) \frac{df_m^{-1}(y)}{dy}. \quad (13)$$

This is a counterpart of (5). Now, note that (4) is valid irrespective of the form of $T(y|x)$. Then, substituting (13) into that equation, we find the counterpart of (6)

$$\sum_{m=1}^M a_m \left[N_1 \left(f_m^{-1}(\bar{y}) \right) - N_0 \left(f_m^{-1}(\bar{y}) \right) \right] \frac{df_m^{-1}}{dy} \Big|_{y=\bar{y}} = 0. \quad (14)$$

Let us denote

$$\bar{x}_m \equiv f_m^{-1}(\bar{y}) \quad (15)$$

(see Fig. 4). Since according to (12a), all $df_m^{-1}/dy > 0$, then the sign of the terms in the square brackets in (14) must change as m changes from 1 to M . That is, there is an index $m_0 < M$ such that

$$\begin{aligned} N_1(\bar{x}_m) &\geq N_0(\bar{x}_m), & m \leq m_0 \\ N_1(\bar{x}_m) &< N_0(\bar{x}_m), & m > m_0. \end{aligned} \quad (16)$$

For example, $m_0 = 2$ in Fig. 2. Alternatively, one can write that

$$\begin{aligned} \bar{x}_m &\geq \bar{x}, & m \leq m_0 \\ \bar{x}_m &< \bar{x}, & m > m_0 \end{aligned} \quad (17)$$

where \bar{x} is defined in (2). Inequalities (17) along with (15) are the sought counterpart of (7). We now substitute (13) and (15) into (3) to obtain

$$\text{BER}_y = \sum_{m=1}^M a_m \left(\frac{1}{2} \int_0^{\bar{x}_m} N_1(x) dx + \frac{1}{2} \int_{\bar{x}_m}^{\infty} N_0(x) dx \right). \quad (18)$$

By virtue of (2) and (17), there can be at most one term in parentheses in (18) that equals the r.h.s. of (1), while all the other terms satisfy

$$\frac{1}{2} \left(\int_0^{\bar{x}_{(m)}} N_1(x) dx + \int_{\bar{x}_{(m)}}^{\infty} N_0(x) dx \right) > \frac{1}{2} \left(\int_0^{\bar{x}} N_1(x) dx + \int_{\bar{x}}^{\infty} N_0(x) dx \right) \equiv \text{BER}_x. \quad (19)$$

Substituting (19) into (18) and using the normalization condition for $a_{(m)}$ from (11), we obtain (10), as desired.

This derivation clearly shows the reason behind the BER degradation after a regenerator whose response consists of several transfer curves, as in (11). This reason is that, in view of (16), all (except at most one) of the “partial thresholds” $\bar{x}_{(m)}$ are suboptimal for “their” transfer curves and, hence, contribute a greater probability of error to the BER_y than the unique optimal threshold \bar{x} would do. For $T(y|x)$ of a general form, i.e., not restricted to (11), the mechanism of the BER degradation is the same spread of “partial thresholds,” as we will now show formally.

C. Proof of (10) for a General $T(y|x)$

The mathematical trick for this proof is to represent a general $T(y|x)$ in a form analogous to (11)

$$T(y|x) = \int_0^{\infty} \alpha(\mu) \delta(y - \phi(x, \mu)) d\mu \quad (20)$$

where $\phi(x, \mu)$ is any function satisfying, for all $x, \mu > 0$

$$\partial\phi(x, \mu)/\partial x > 0 \quad (21a)$$

$$\partial\phi(x, \mu)/\partial\mu > 0 \quad (21b)$$

and $\alpha(\mu)$ must satisfy the normalization condition

$$\int_0^{\infty} \alpha(\mu) d\mu = 1. \quad (22)$$

Conditions (21) are counterparts of conditions (12), and condition (22) is a counterpart of the last equation in (11). In Appendix we prove that given any $T(y|x)$ satisfying (9), representation (20)–(22) can always be (explicitly) found. Let us also note that the formally introduced quantity μ in (20) can be interpreted as, e.g., the width or any other continuous parameter(s) characterizing the temporal shape of the input pulse.

We are now just a short step away from proving (10) for a general $T(y|x)$. First, however, we need to introduce yet another piece of notation: If $y = \phi(x, \mu)$, then $x = \phi^{(-1, \cdot)}(y, \mu)$ denotes the inverse of ϕ with respect to x while keeping μ fixed. This $\phi^{(-1, \cdot)}(y, \mu)$ is guaranteed to exist by condition (21a).

Let us substitute (20) into (8) to obtain

$$R_k(y) = \int_0^{\infty} \alpha(\mu) N_k \left(\phi^{(-1, \cdot)}(y, \mu) \right) \frac{\partial\phi^{(-1, \cdot)}(y, \mu)}{\partial y} d\mu. \quad (23)$$

This is the counterpart of (13). Substituting (23) into (3), we obtain

$$\text{BER}_y = \frac{1}{2} \int_0^{\infty} d\mu \alpha(\mu) \cdot \left[\int_0^{\bar{y}} N_1 \left(\phi^{(-1, \cdot)}(y, \mu) \right) \frac{\partial\phi^{(-1, \cdot)}(y, \mu)}{\partial y} dy + \int_{\bar{y}}^{\infty} N_0 \left(\phi^{(-1, \cdot)}(y, \mu) \right) \frac{\partial\phi^{(-1, \cdot)}(y, \mu)}{\partial y} dy \right]. \quad (24)$$

Introducing a notation analogous to (15)

$$\bar{x}(\mu) = \phi^{(-1, \cdot)}(\bar{y}, \mu) \quad (25)$$

we rewrite (24) as the following counterpart of (18):

$$\begin{aligned} \text{BER}_y &= \int_0^{\infty} d\mu \alpha(\mu) \cdot \left[\frac{1}{2} \int_0^{\bar{x}(\mu)} N_1(x) dx + \frac{1}{2} \int_{\bar{x}(\mu)}^{\infty} N_0(x) dx \right] \\ &> \int_0^{\infty} d\mu \alpha(\mu) \cdot \text{BER}_x \\ &= \text{BER}_x \end{aligned} \quad (26)$$

which proves (10). Here we have used (22). The “>” sign in (26) holds because at most one $\bar{x}(\mu)$ out of the continuum equals \bar{x} and, thus, yields a term in the square brackets that equals BER_x , whereas all the remaining values of μ contribute more than BER_x .

III. DISCUSSION

A. Extension of the Main Result to a Realistic Regenerator, and Implications for Regenerator Chains

In Section II, we established the BER degradation under the restrictive assumption that the regenerator transforms ZEROs and ONES in exactly the same way, so that $T(y|x)$ is the same for these two logical symbols. In reality, $T_1(y|x) \neq T_0(y|x)$ in general. (Here, as before, we use subscripts without parentheses to label quantities pertaining to ONES and ZEROs.) Examples of such distinct transfer bands of ONES and ZEROs for a particular regenerator can be found in Fig. 6 of [10] [Fig. 3 here corresponds to Fig. 6(b) in [10]] and in Fig. 7 below. We will now argue that even if $T_1(y|x)$ and $T_0(y|x)$ are different but overlap significantly, the BER is still degraded after the regenerator in question. Given that this argument must necessarily be qualitative (since it would be problematic to quantify the word “significantly” in the previous sentence), we will present it only for the case where each of $T_1(y|x)$ and $T_0(y|x)$ are given by (11). To simplify the details, but still without loss of generality, we will further assume that all curves $f_{(m)}(x)$ are the same for ONES and ZEROs, but $a_{1,(m)} \neq a_{0,(m)}$ in general. This setup is illustrated in Fig. 5, where $M = 4$ and $a_{1,(1)} = 0$, $a_{0,(4)} = 0$. Precise relations among $a_{1,(2)}$ through $a_{1,(4)}$ and $a_{0,(1)}$ through $a_{0,(3)}$ are not important for our qualitative argument.

Proceeding as in Section II-B, one obtains the following generalization of (18):

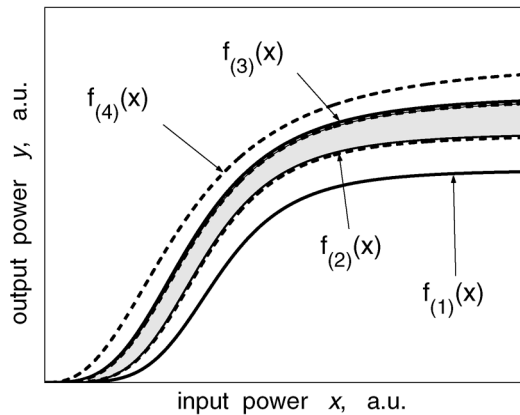


Fig. 5. Schematics of different, but overlapping transfer bands $T_1(y|x)$ and $T_0(y|x)$ that consist of discrete transfer curves $f_{(m)}$. Dashed (solid) lines show the transfer curves for ONEs (ZEROs).

$$\text{BER}_y = \sum_{m=1}^M \frac{1}{2} \cdot \left(a_{1,(m)} \int_0^{\bar{x}_{(m)}} N_1(x) dx + a_{0,(m)} \int_{\bar{x}_{(m)}}^{\infty} N_0(x) dx \right). \quad (27)$$

Let us denote, for each m

$$\underline{a}_{(m)} = \min(a_{1,(m)}, a_{0,(m)}), \quad \Delta a_{k,(m)} = a_{k,(m)} - \underline{a}_{(m)}$$

so that

$$\Delta a_{k,(m)} \geq 0 \quad \text{for } k = 0, 1, \quad m = 1, \dots, M. \quad (28)$$

Then (27) is rewritten as

$$\text{BER}_y = \sum_{m=1}^M \frac{1}{2} \cdot \left[\underline{a}_{(m)} \left(\int_0^{\bar{x}_{(m)}} N_1(x) dx + \int_{\bar{x}_{(m)}}^{\infty} N_0(x) dx \right) + \left(\Delta a_{1,(m)} \int_0^{\bar{x}_{(m)}} N_1(x) dx + \Delta a_{0,(m)} \int_{\bar{x}_{(m)}}^{\infty} N_0(x) dx \right) \right]. \quad (29)$$

In view of (28), the term in the last line of (29) is always positive. For each m , the terms in parentheses in the second line (multiplied by $1/2$) are greater than BER_x [see (19)]. Moreover, since the BER is highly sensitive to the choice of the threshold (note the scale of the vertical axis in Fig. 2), those terms are *much* greater than BER_x . On the other hand, $\sum_{m=1}^M \underline{a}_{(m)}$ is less, but *not much less*, than unity, which is a quantitative way to express our assumption that the overlap between $T_1(y|x)$ and $T_0(y|x)$ is “significant.” Thus, in such a case, the BER after the regenerator is still likely to be worse than that before it.

Let us note that this conclusion agrees with numerical results of [10]. Namely, the transfer band for ZEROs shown in Fig. 6(a) of [10] was, on average, lower than the transfer band for ONEs (similarly to what is depicted in Fig. 5 of this paper). Yet, the numerically computed BER was still degraded by the regenerator (see [10, Fig. 3(a)]).

While, as explained above, it is not possible to access the BER degradation quantitatively, it is still possible to predict that this degradation should worsen with lowering the BER of the input signal. Indeed, the probability density for ONEs before the regenerator typically gets steeper into its left tail (see Fig. 2), where the decision threshold is. (The steeper the probability density, the more a spread in the “partial thresholds” $\bar{x}(\mu)$ will affect the BER.)

This stronger degradation of lower error probabilities should have significant impact on the BER calculations for chains of regenerators. Indeed, in such chains, the error probability after the first few regenerators is very low (see, e.g., [15]), so it will be most strongly degraded. On the other hand, regenerators closest to the receiver will not be able to efficiently suppress pulse distortions because the latter may already be too large; in fact, the last regenerator in the chain may even degrade the BER of the received signal if placed too close to the receiver, as we showed in this work. Thus, it may be relevant to consider the problem of optimizing the locations of regenerators along the transmission line. It should be noted that such an optimization will strongly depend on the type of the signal impairments that takes place in the specific transmission system [12]. For a system limited by the optical signal-to-noise ratio (OSNR), the problem of the optimal placement of a single regenerator was considered in [8]. However, there, as in other papers on regenerator chains (see, e.g., [16] and references therein), the regenerator was modeled by its static transfer curve. In general, the main result of the present work—i.e., that the regenerator necessarily degrades the BER—suggests that the benefit of regenerators is more modest than predicted in those papers, where the transfer-curve-based calculations implied that the regenerators did not change the BER.

B. Manifestation of BER Degradation in Other Signal-Reshaping Processors

As we noted in the Introduction, wavelength converters whose operation is based on nonlinear propagation in fibers or semiconductors is another group of signal processors that exhibit noninstantaneous response. Consequently, one should expect that they, also, degrade the BER. This is confirmed by the BER curves reported in [4]–[7] for wavelength converters utilizing four different operation principles.

These papers give reasons for the BER degradation that do not refer to noninstantaneous response of the device. However, one can see that in all those cases, the converted signal will depend not only on the input power or width of the input signal, but also on its temporal shape, which is a manifestation of the noninstantaneous response. For example, many authors (see, e.g., [5], [6], [10], and [14]) mention the importance of placing a band-pass filter in front of the signal processor to limit the amount of optical noise entering the device. In particular, in [10], it was shown via numerical simulations that the wider the bandwidth of this filter, the greater the BER degradation incurred by the processor (a regenerator, in this case). This phenomenon has a simple explanation in the light of the result proved here. Indeed, the wider the bandwidth of the noise allowed into the regenerator, the greater the variations of the temporal shape of the signal degraded by such noise. This implies a “fatter” transfer band

$T(y|x)$, which, in its turn, leads to a greater spread of “partial thresholds” $\bar{x}(\mu)$ (see Section II) and, thus, to a greater BER degradation.

Let us note that the BER must also be degraded by a signal processor with noninstantaneous response operating not in optical, but in electronic domain. An example here may be a limiting amplifier, which is used at the front end of a receiver. Its static transfer curve resembles that of a regenerator (see Fig. 1). Receiver designers try to make the bandwidth of the limiting amplifier as wide as possible to avoid distortion of high-frequency components of the signal. As is well known, a wide bandwidth translates into a very short response time of the device. In other words, the response of the limiting amplifier must be sufficiently fast (i.e., “almost instantaneous”) in order to avoid BER degradation. This agrees with the main result proved in this paper.

C. Why the BER can be Improved by a Timing- or Phase-Restoring Processor

The preceding considerations pertain to *phase-insensitive* (see the end of this subsection) signal-reshaping processors, which affect the signal’s power. One prominent example of this kind of processor is the Mamyshev regenerator [1], based on spectral broadening and off-center filtering. When the receiver’s optical filter is reasonably close to the optimal, i.e., matched, filter, such signal-reshaping processors have no mechanism to distinctly discriminate a ONE that “went below” the decision threshold from a ZERO that “went above” it due to noise or other distortions. In this case, the transfer bands of ONES and ZEROs significantly overlap (see Fig. 3), which leads to the BER degradation as explained in Section III-A.

Regenerators that retiming the signal are also unable to discriminate between a ONE that is “too short” and a ZERO that is “too tall.” Hence, they also cannot eliminate *this* type of error. Now, consider a ONE that is displaced from its time slot but whose peak power is well above the decision threshold. Before retiming, such a ONE is detected as a ZERO since at the detection instance, its power is measured at the pulse’s “tail” and, hence, is too low. However, after proper retiming, the peak of this pulse will occur near the decision instance, and, hence, the pulse will be correctly detected as a ONE. On the other hand, ZEROs may occur anywhere within the bit slot, so retiming does not, in general, increase the probability to detect a ZERO incorrectly. Thus, overall, the BER is improved by proper retiming. In terms of transfer bands, the retiming processor “raises” the left end of the ONES’ band (which is where the decision threshold is; see, e.g., Fig. 3) well above the left end of the ZEROs’ band.

The benefit of retiming processors is, of course, well known, and we included this discussion here merely to avoid possible confusion with the main result of this paper. The simplest retiming processor is just a section of dispersion-compensating fiber in front of the receiver. More sophisticated signal retimers were considered in [17], [18]. Let us note that since a 3R (2R plus retiming) regenerator performs both reshaping and retiming of the signal, the BER at its output *may*, in principle, be improved. Whether this improvement actually occurs for a particular degraded signal, would depend on the balance between the BER degradation due to reshaping and its improvement due

to retiming. In other words, the change of the BER is a function of the kind of signal degradation (i.e., the amplitude or timing jitter) rather than a function of the particular device. As before, this BER change can be estimated by plotting the transfer bands for ONES and ZEROs: if they significantly overlap, the BER is most likely degraded; if, on the other hand, most of the ONES’ band lies higher than most of the ZEROs’ band, the BER is likely improved.

We can also use the analogy between the temporal position of the pulse and its phase at the detection moment (see, e.g., [19]) to conclude that phase-restoring processors placed in front of the receiver can improve the BER of phase-shift-keyed signals. Such BER improvement was demonstrated numerically in [19], [20], and experimentally in [21].

Finally, let us point out a simple phase-restoring processor that is routinely used to improve the BER of *amplitude*-shift-keyed signals. This processor is a linear dispersive fiber, already mentioned in relation to its retiming functionality. As is well known, it is also used to transform chirped pulses into chirp-free ones, which makes the pulses “taller” and thereby improves the BER. This well-known fact may seem to contradict the main result of this paper. Indeed, a linear dispersive fiber has noninstantaneous response (i.e., its output depends on the *shape* of the input). Then, how can it discriminate between ONES and ZEROs having the same spectral bandwidth?

To resolve this seeming contradiction, let us write down the fields $z(t)$ and $o(t)$ of the ZEROs and chirped ONES, respectively, at the input to the fiber: $z_{\text{in}}(t) = n_{1,\text{in}}(t)$, $o_{\text{in}}(t) = s_{\text{chirped}}(t) + n_{2,\text{in}}(t)$, where $n_{\{1,2\},\text{in}}(t)$ are the noise fields and $s_{\text{chirped}}(t)$ is the field of the chirped signal without noise. (The noise fields $n_{1,\text{in}}(t)$ and $n_{2,\text{in}}(t)$ are independent of one another but otherwise have the same statistics.) The phases of the signal $s_{\text{chirped}}(t)$ and of a typical ZERO (i.e., $n_{1,\text{in}}(t)$) that is “tall” enough to cause an error at the receiver are shown in Fig. 6. While the signal’s phase is nearly parabolic, the noise’s phase has random slope and curvature. This is also true about the phase of the other noise field $n_{2,\text{in}}(t)$. At the output of the dispersive fiber, the ZERO’s and ONE’s fields are: $z_{\text{out}}(t) = n_{1,\text{out}}(t)$, $o_{\text{out}}(t) = s_{\text{chirp-free}}(t) + n_{2,\text{out}}(t)$. The phases of $s_{\text{chirp-free}}$ and a typical $n_{1,\text{out}}$ are shown in Fig. 6. Thus, the fiber makes the signal “taller” while it does *not*, in general, make the noise fields “taller.” In fact, our numerical experiments show that, on average, it makes them lower. In terms of transfer bands, this means that the ONES’ band is raised and the ZEROs’ band is lowered, as shown in Fig. 7. The corresponding probability densities are shown in Fig. 8, which confirms the well-known fact that a properly chosen linear dispersive fiber indeed improves the BER of a chirped signal.

IV. CONCLUSION

In Section II of this paper, we showed that under a certain conditions, a signal-reshaping processor whose output depends on the temporal shape of the input signal, rather than just on its power, degrades the signal BER. Specifically, let x be the signal power obtained if the receiver is placed in front of the processor. Then the received power y of the signal after the processor can be found anywhere within some distribution $T(y|x)$, depending on the shape of the input. Now, let BER_x be the

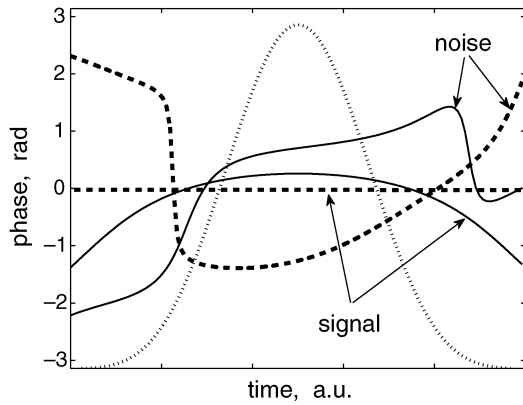


Fig. 6. Phases of the noiseless signal and a typical noise sample (i.e., a ZERO) whose amplitude is near the decision threshold, at the input (thin solid) and output (thick dashed) of a linear dispersive fiber. The fiber provides 200 ps/nm of dispersion to exactly compensate for the chirp of the input signal. The OSNR in one polarization within 0.1 nm is 17 dB. Limiting the noise bandwidth is a third-order Gaussian filter with the optical bandwidth of 33 GHz at full width at half maximum (FWHM). The noiseless signal is a Gaussian pulse with the FWHM of 32 ps before the optical filter; its power profile is shown by the dotted line. The ZERO in this figure, as well as the results shown in Figs. 7 and 8 below, are obtained by a method described in [10].

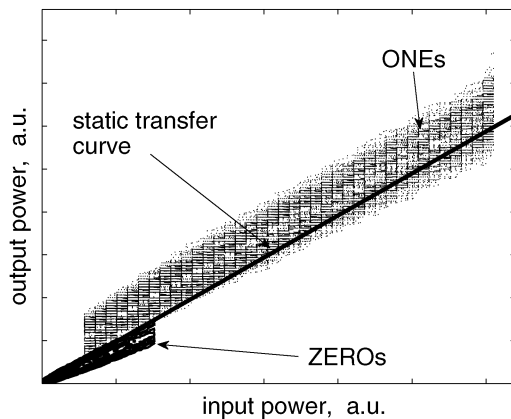


Fig. 7. The transfer bands for ONEs and ZEROs for the conditions listed in the caption for Fig. 6. No electrical filter is used at the receiver.

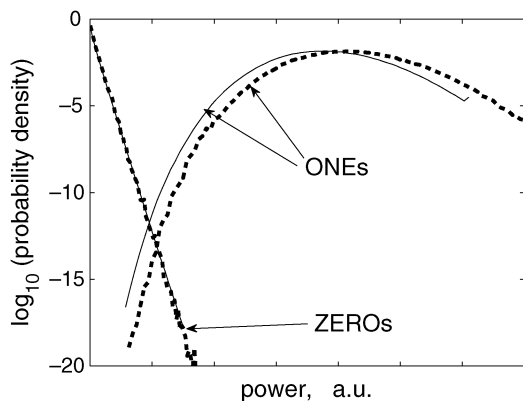


Fig. 8. The probability densities for ONEs and ZEROs at the input (thin solid) and output (thick dashed) of a linear dispersive fiber. All parameters are as listed in the captions for Figs. 6 and 7. The BERs at the input and output are about $5 \cdot 10^{-12}$ and $2 \cdot 10^{-13}$, respectively.

signal BER obtained if the receiver is placed in front of the processor. Assume that the processor transforms logical ONEs and

ZEROs in exactly the same way. (That is, $T_1(y|x) = T_0(y|x)$, i.e., the processor does not distinguish between these two symbols, as would occur if the signal has been sent through the matched filter before being processed.) Let BER_y be the BER measured when the receiver is placed immediately after the processor (i.e., no noise is added to the processor's output). Then $\text{BER}_y > \text{BER}_x$.

A realistic processor would transform input ZEROs and ONEs differently, since the matched filter is not achievable in practice. Then, $T_1(y|x) \neq T_0(y|x)$. However, a realistic filter is designed to approach the performance of the matched one, and, therefore, $T_1(y|x)$ and $T_0(y|x)$ overlap significantly. In Section III-A, we argued that under this, realistic, condition, the processor still degrades the BER. We also explained that this degradation should be more prominent for lower values of the input BER.

Our discussion was mostly focused on all-optical regenerators. In particular, our main result provides a theoretical foundation for the numerically observed BER degradation in the semiconductor-optical-amplifier-based [3] and fiber-based Mamyshev-type [10] 2R regenerators. It should be stressed, however, that the BER is degraded if the receiver were placed *immediately* after the regenerator. If the regenerators (or even a single such device [8]) is placed in the transmission line so that noise and other distortions accumulate between them and the receiver, such a chain of regenerators can still improve the BER [8], [10]–[12], [15].

We pointed out, in Section III-B, that the BER is also degraded by other signal-reshaping processors, both in optical (e.g., wavelength converters) and electronic (limiting amplifier) domains, if the response of those devices is slower than, or comparable to, variations of the temporal profile of the input signal.

Finally, in Section III-C, we explained that the well-known fact of the BER improvement by processors restoring the signal's timing or phase (for both phase- and amplitude-shift-keyed transmission) does not contradict our main result, which is that the BER is generically degraded by signal-reshaping processors.

APPENDIX

Here, we show that given any $T(y|x)$ satisfying (9), one can find a function $\phi(x, \mu)$ satisfying (21) and a function $\alpha(\mu)$ satisfying (22) such that (20) holds.

Similarly to the notation introduced before (23), let us define $\phi^{(-1)}(x, y)$ to be the inverse of $y = \phi(x, \mu)$ with respect to μ while keeping x fixed. The existence of such an inverse is guaranteed by condition (21b). Thus, if $y = \phi(x, \mu)$, then $\mu = \phi^{(-1)}(x, y)$. For example, function

$$y \equiv \phi(x, \mu) = \frac{x\mu}{1 + x} \quad (\text{A1})$$

satisfies both conditions (21), and also $y < \mu$. The inverses $\phi^{(-1)}(y, \mu)$ and $\phi^{(-1)}(x, y)$ are then

$$x \equiv \phi^{(-1)}(y, \mu) = \frac{y}{\mu - y}, \quad \mu \equiv \phi^{(-1)}(x, y) = \frac{y}{x} + y. \quad (\text{A2})$$

This example shows that at least one function $\phi(x, \mu)$ satisfying conditions (21) exists; in fact, there is a continuum of such functions. Let us select one of them and use it in what follows. Then the integration of (20) yields

$$\alpha(\phi^{(-1)}(x, y)) = T(y|x) / \left(\frac{\partial \phi^{(-1)}(x, y)}{\partial y} \right)$$

or, equivalently

$$\alpha(\mu) = T(x, \phi(x, \mu)) \frac{\partial \phi(x, \mu)}{\partial \mu}. \quad (\text{A3})$$

This proves that a function $\alpha(\mu)$ in (20) can be explicitly found given $T(y|x)$ and $\phi(x, \mu)$. It remains to show that this $\alpha(\mu)$ satisfies (22). This follows straightforwardly by acting on (A3) with $\int_0^\infty d\mu$ and using (9).

ACKNOWLEDGMENT

The author would like to thank the anonymous referee whose comments prompted the clarification (see Section III-C) of how, in light of the main result of this paper, a linear dispersive fiber can improve the BER.

REFERENCES

- [1] P. V. Mamyshev, "All-optical regeneration based on self-phase modulation effect," in *Proc. 24th Eur. Conf. Optical Communications*, Sep. 20–24, 1998, vol. 1, pp. 475–476.
- [2] M. Matsumoto, "Analysis of optical regeneration utilizing self-phase modulation in a highly nonlinear fiber," *IEEE Photon. Technol. Lett.*, vol. 14, no. 3, pp. 319–321, Mar. 2002.
- [3] F. Öhman, S. Bischoff, B. Tromborg, and J. Mørk, "Noise and regeneration in semiconductor waveguides with saturable gain and absorption," *IEEE J. Quant. Electron.*, vol. 40, no. 3, pp. 245–255, Mar. 2004.
- [4] J. Yu and P. Jeppesen, "80-Gb/s wavelength conversion based on cross-phase modulation in high-nonlinearity dispersion-shifted fiber and optical filtering," *IEEE Photon. Technol. Lett.*, vol. 13, no. 8, pp. 833–835, Aug. 2001.
- [5] N. Chi, L. Xu, K. S. Berg, T. Tokle, and P. Jeppesen, "All-optical wavelength conversion and multichannel 2R regeneration based on highly nonlinear dispersion-imbalanced loop mirror," *IEEE Photon. Technol. Lett.*, vol. 14, no. 11, pp. 1581–1583, Nov. 2002.
- [6] W. Mao, P. A. Andrekson, and J. Toulouse, "All-optical wavelength conversion based on sinusoidal cross-phase modulation in optical fibers," *IEEE Photon. Technol. Lett.*, vol. 17, no. 2, pp. 420–422, Feb. 2005.
- [7] J. Ma, J. Yu, C. Yu, Z. Jia, X. Sang, Z. Zhou, T. Wang, and G. K. Chang, "Wavelength conversion based on four-wave mixing in high-nonlinearity dispersion-shifted fiber using a dual-pump configuration," *J. Lightw. Technol.*, vol. 24, no. 7, pp. 2851–2858, Jul. 2006.

- [8] B. Charbonnier, N. El Dahdah, and M. Joindot, "OSNR margin brought about by nonlinear regenerators in optical communication links," *IEEE Photon. Technol. Lett.*, vol. 18, no. 3, pp. 475–477, Feb. 2006.
- [9] M. Rochette, L. Fu, V. Ta'eed, D. J. Moss, and B. J. Eggleton, "2R optical regeneration: An all-optical solution for BER improvement," *IEEE J. Sel. Topics Quant. Electron.*, vol. 12, no. 4, pp. 736–744, Jul.–Aug. 2006.
- [10] T. I. Lakoba, "Multicanonical Monte Carlo study of the BER of an all-optically 2R regenerated signal," *IEEE J. Sel. Topics Quant. Electron.*, vol. 14, no. 3, pp. 599–609, May–Jun. 2008.
- [11] S. Bischoff, B. Lading, and J. Mørk, "BER estimation for all-optical regenerators influenced by pattern effects," *IEEE Photon. Technol. Lett.*, vol. 14, no. 1, pp. 33–35, May 2002.
- [12] M. Karlsson, H. Sunnerud, and B.-E. Olsson, "PMD compensation using 2R and 3R regenerators," presented at the 30th Eur. Conf. Optical Communications, Sep. 5–9, 2004, Paper WE1.4.2.
- [13] M. Rochette, J. N. Kutz, J. L. Blows, D. Moss, T. J. Mok, and B. J. Eggleton, "Bit-error-ratio improvement with 2R optical regenerators," *IEEE Photon. Technol. Lett.*, vol. 17, no. 4, pp. 908–910, Apr. 2005.
- [14] T. N. Nguyen, M. Gay, L. Bramerie, T. Chartier, J.-C. Simon, and M. Joindot, "Noise reduction in 2R-regeneration technique utilizing self-phase modulation and filtering," *Opt. Exp.*, vol. 14, no. 5, pp. 1737–1747, Mar. 2006.
- [15] P. Öhlén and E. Berglind, "Noise accumulation and BER estimates in concatenated nonlinear optoelectronic repeaters," *IEEE Photon. Technol. Lett.*, vol. 9, no. 7, pp. 1011–1013, Jul. 1997.
- [16] M. R. G. Leiria and A. V. T. Cartaxo, "Impact of the signal and nonlinearity extinction ratios on the design of nonideal 2R all-optical regenerators," *J. Lightw. Technol.*, vol. 26, no. 2, pp. 276–285, Jan. 2008.
- [17] L. F. Mollenauer and C. Xu, "Time-lens timing jitter compensator in ultra-long haul DWDM dispersion-managed soliton transmissions," presented at the Conf. Lasers and Electro-Optics, Long Beach, CA, 2002, paper CPDB1.
- [18] I. O. Nasieva, S. Boscolo, and S. K. Turitsyn, "Bit error rate improvement by nonlinear optical decision element," *Opt. Lett.*, vol. 31, no. 9, pp. 1205–1207, May 2006.
- [19] X. Liu, X. Wei, R. Slusher, and C. J. McKinstrie, "Improving transmission performance in differential phase-shift-keyed systems by use of lumped nonlinear phase shift compensation," *Opt. Lett.*, vol. 27, no. 18, pp. 1616–1618, Sep. 2002.
- [20] C. Xu and X. Liu, "Postnonlinearity compensation with data-driven phase modulators in phase-shift-keying transmission," *Opt. Lett.*, vol. 27, no. 18, pp. 1619–1621, Sep. 2002.
- [21] G. Zhu, L. Mollenauer, and C. Xu, "Experimental demonstration of postnonlinearity compensation in a multispan DPSK transmission," *IEEE Photon. Technol. Lett.*, vol. 19, no. 9, pp. 1007–1009, May 2006.

Taras I. Lakoba received the Diploma in physics from Moscow State University, Moscow, Russia, in 1989, and the Ph.D. degree in applied mathematics from Clarkson University, Potsdam, NY, in 1996. His Ph.D. dissertation was devoted to perturbations and stability of solitary waves in nonlinear optics.

In 2000, he joined the Optical Networking Group, Lucent Technologies, where he was engaged in the development of an ultralong-haul dense wavelength-division-multiplexing (DWDM) terrestrial transmission system. Since 2003, he has been with the Department of Mathematics and Statistics, University of Vermont, Burlington, VT, where he is currently an Assistant Professor. His current research interests include multichannel all-optical 2R regeneration, the effect of noise in optical communication systems, numerical methods for obtaining stationary solutions of nonlinear wave equations, and perturbation techniques.